

Latest developments in resonantly diode-pumped Er:YAG lasers

Igor Kudryashov^{a)} and Dmitri Garbuzov

Princeton Lightwave Inc., 2555 US Route 130, Cranbury, New Jersey, 08512

Mark Dubinskii

U.S. Army Research Laboratory, AMSRD-ARL-SE-EO, 2800 Powder Mill Road, Adelphi, Maryland 20783

ABSTRACT

Significant performance improvement of the Er(0.5%):YAG diode pumped solid state laser (DPSSL) has been achieved by pump diode spectral narrowing via implementation of an external volumetric Bragg grating (VBG). Without spectral narrowing, with a pump path length of 15 mm, only 37% of 1532 nm pump was absorbed. After the VBG spectral narrowing, the absorption of the pumping radiation increased to 62 - 70%. As a result, the incident power threshold was reduced by a factor of 2.5, and the efficiency increased by a factor of 1.7, resulting in a slope efficiency of ~23 - 30%. A maximum of 51 W of CW power was obtained versus 31 W without the pump spectrum narrowing. More than 180 mJ QCW pulse output energy was obtained in a stable-unstable resonator configuration with a beam quality of $M^2 = 1.3$ in the stable direction and $M^2 = 1.1$ in the unstable direction. The measured slope efficiency was 0.138 J/J with a threshold energy of 0.91 J.

Keywords: Er:YAG, diode-pumped, volumetric Bragg grating, solid-state lasers.

1. INTRODUCTION

Growing interest in high power lasers in the eye-safe spectral domain has initiated a new wave of activity in developing solid-state lasers based on Er³⁺-doped materials. Er³⁺:YAG has good mechanical, thermal and thermo-optic properties and is one of the most attractive active materials for developing ~1.6- μ m eye-safe SSLs. Most importantly, it has a resonantly-pumped operation mode very similar to, and in some ways better than, Yb:YAG lasers. Spectroscopy of 1450 \leftrightarrow 1660-nm transitions between the ⁴I_{13/2} and ⁴I_{15/2} Stark-split manifolds in Er³⁺:YAG, forming a quasi-three level system (see Fig. 1), has been studied by numerous scientific groups (e.g., [1,2]). Four upper states of the eight Stark components of the ground ⁴I_{15/2} manifold serve as the terminal states for Er³⁺ laser transitions with the wavelengths ranging from 1617 to 1660 nm. Compared to co-dopant assisted excitation used for pumping (Yb,Er):YAG-based SSLs, a major advantage of the Er:YAG resonant pumping into 1470 and 1532 nm bands is a low quantum defect. It allows for shifting a significant part of thermal load from the Er-doped gain medium itself to the pump diodes, thus greatly reducing gain medium thermal distortions deleterious to SSL power scaling with high beam quality. Recently

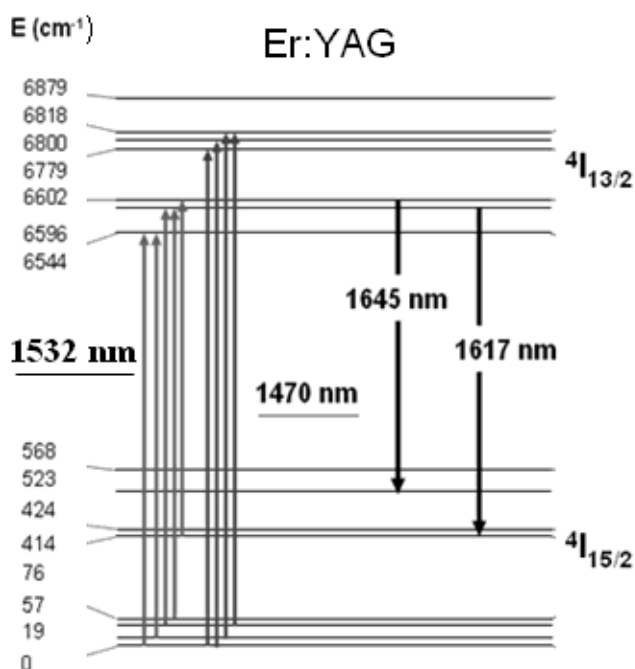


Fig. 1. Er³⁺:YAG energy levels along with absorption and emission transitions in the 1.45 - 1.66 μ m spectral range.

^{a)} E-mail: ikoudriachov@princetonlightwave.com

significant progress has been made in the development of resonantly-pumped Er:YAG SSL with Er-fiber lasers as well as direct diode pumping [3-5]. Due to dramatic strides made in Quantum Well Separate Confinement Heterostructure (QW SCH) lasers based on InGaAsP/InP systems [6,7], direct diode pumping can deliver impressive efficiency results which are highly competitive with those obtained with Er-fiber laser pumping. The majority of the problems with pumping Er:YAG by InP laser diodes are associated with the pump spectral width being much wider than the spectral width of GaAs-based laser diodes used for (Yb,Er):YAG pumping. Optimization of InP laser diode design [7] has allowed for the reduction of the pump output spectrum full width at half maximum (FWHM), but this spectral width is still too wide to match individual Er:YAG absorption lines. One of the most promising approaches to appropriate InP diode spectral narrowing consists in using the volumetric Bragg grating (VBG) as a highly efficient selective feedback element [8]. Reported here is significant performance improvement of the Er(0.5%):YAG DPSSL, which was achieved by pump diode spectral narrowing via the implementation of an external Bragg grating. 51 W of CW Er:YAG power was achieved versus 31 W without the pump spectrum narrowing.

2. EXPERIMENT

A 0.5% Er:YAG slab was used in our experiments. A low doping level was chosen to minimize Er^{3+} upconversion losses [9]. A laser slab of dimensions $60 \times 15 \times 2.5 \text{ mm}^3$ was In-bonded to a water-cooled copper heatsink. All measurements were done with a cooling water temperature of $\sim 15^\circ\text{C}$. The two $2.5 \times 60 \text{ mm}^2$ sides were polished and had antireflective coatings ($R < 0.2\%$) at 1645 nm. 1530-nm single 1-cm laser diode arrays, as well as stacks of seven or ten of these arrays, mounted on microchannel coolers (pitch 1.8 mm) were used for pumping. Each array was fast-axis and slow-axis collimated (FAC and SAC). A schematic of the CW ten-diode-array-stack pumped Er^{3+} :YAG laser setup is shown in Fig. 2. Figure 2a demonstrates pump ray-tracing results in the slab plane. Figures 2b and 2c (detailed slab view) demonstrate pump ray-tracing results in the plane perpendicular to the slab. Two cylindrical lenses with focal lengths of 100 and 30 mm were used to launch pump radiation into the slab through the dichroic mirror M1. The laser cavity comprised two flat mirrors M1 ($>99.8\%$ @ 1645nm) and M2 (output coupler), and the total cavity length was 50 mm. Output couplers with reflectivities of 98%, 96%, 93% and 85% were used in order to optimize laser performance. The DPSSL was tested with and without diode spectral narrowing by VBG.

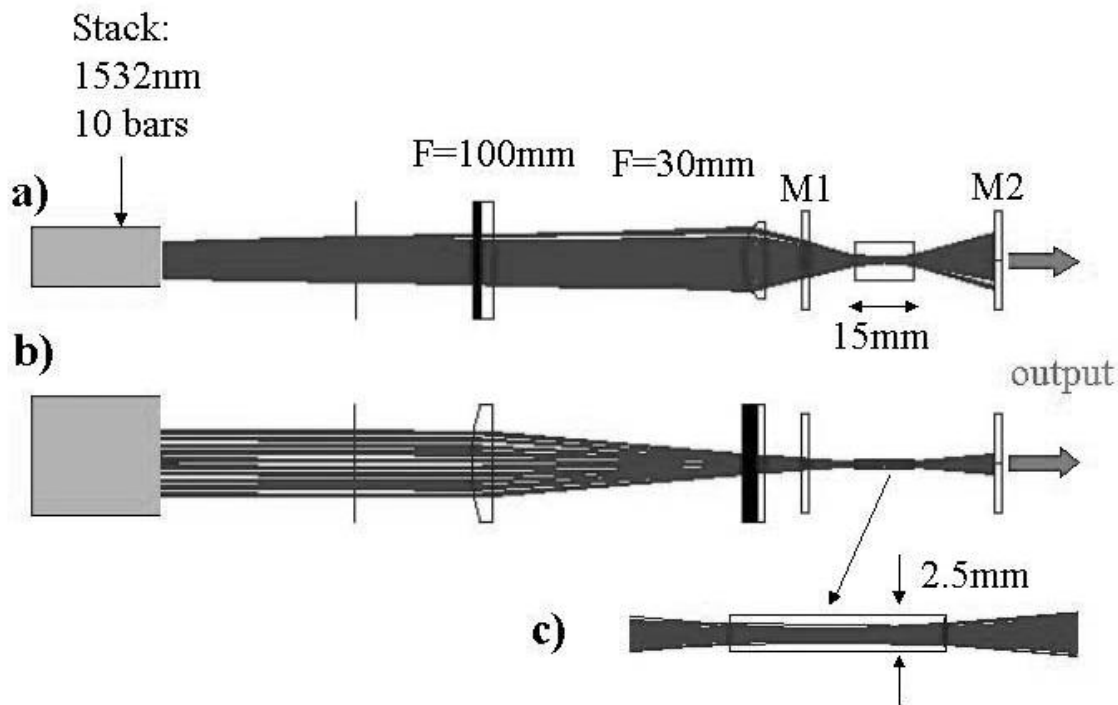


Fig. 2. Schematic view of SSL: a) pump ray-tracing in the slab plane; b) pump ray-tracing for the ten-array stack in the plane perpendicular to the slab; c) detailed view of pump ray-tracing in the plane perpendicular to the slab.

A VBG with dimensions 23 x 14 x 1.5 mm³ and nominal reflectivity of 20% was supplied by Ondax, Inc. The nominal central wavelength was 1531.5 nm. Heated air flow was used for wavelength fine tuning and stabilization around 1532.5 nm.

For quasi continuous wave (QCW) pumping we used the stable-unstable or hybrid resonator in the INNOSLAB configuration (see Fig. 3) invented by K. Du [10]. This type of resonator has several advantages. In this configuration, the slab has only two polished sides, excluding parasitic modes in the slab. In the plane perpendicular to the slab (stable direction) the slab size is small thus providing effective heat removal. The unstable configuration in the slab plane and the use of large slab sizes allows for high power operation without sacrificing beam quality and mode overlapping ratio.

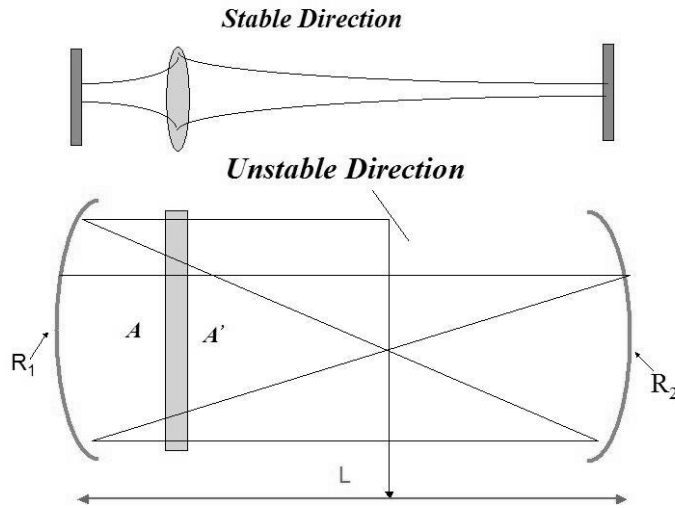


Fig. 3. Hybrid resonator

Output losses (OL) in this resonator are defined by the radii of the cylindrical concave mirrors R1 and R2:

$$OL = 1 - R2/R1$$

For our experiments we used R1 = 365mm and R2 = 339mm, which provided output losses of 7%. The actual resonator had a Γ-shape due to a dichroic mirror at 45 degree between the slab and cylindrical mirror R1. Pump radiation was launched through the dichroic mirror. The seven-array stack with two cylindrical lenses F = 75mm and F = 38mm was employed as a pump source for this configuration.

3. RESULTS AND DISCUSSION

The cross-section of the pump beam from the ten-array stack in the crystal was measured to define the actual dimensions of the gain region. Measurements were carried out in air, but taking into account the ~1.8 refractive index of YAG, we assumed that the beam cross-section measured ~9 mm from the slab front (pump) face corresponds to the actual beam cross-section on the back face. The pump beam was also simulated using the optical design program ZEMAX (Fig. 2). 5mrad x 40mrad divergences for individual arrays were used as simulation parameters. The distribution measured in the back plane of the laser crystal fully confirms the validity of our ZEMAX simulation for the ten-array stack. This good agreement allowed us to use simulated beam profiles for other pump sources (single array and seven-array stack). Estimated beam sizes in the slab are 2.2 mm x 1.7 mm for the ten-array stack, 2.2 mm x 0.6 mm for the single array, and 3.6 mm x 1 mm for the seven-array stack.

The pump incident power and spectra were measured after the dichroic mirror M1 (Fig. 2) to eliminate ambiguities associated with the spectral complexity of the coating. A stable position of the stack spectrum was maintained through control of the temperature of the water through the stack in the entire range of pump currents used, so that with increased stack output power, only pump spectral widening took place. The typical spectrum measured in this location from a stack without a VBG is shown in Fig. 4 (curve 1). One can see that spectral FWHM of the pump is about 9 nm and is much broader than the width of the individual absorption line. Multiple (and overlapping) absorption lines – a “band” – around 1532 nm do help increase the absorbed fraction of the incident power, but from the spectrum taken after the Er³⁺:YAG slab (curve 2) one can see that a significant fraction of the pump power still does not get absorbed.

The VBG-narrowed InGaAsP/InP stack spectra taken before and after the Er³⁺:YAG slab are shown in Fig. 5. The spectra in Fig. 4 and Fig. 5 were measured for the same stack temperature and current through the stack. It can be seen

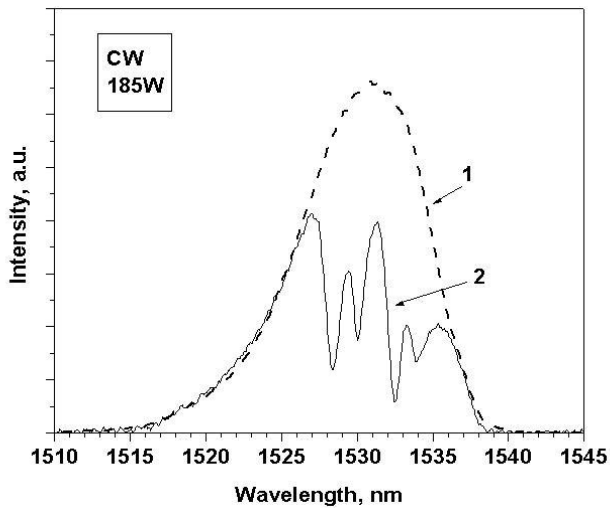


Fig. 4. Pump spectra before (1) and after the slab (2) for the InGaAsP/InP stack without VBG

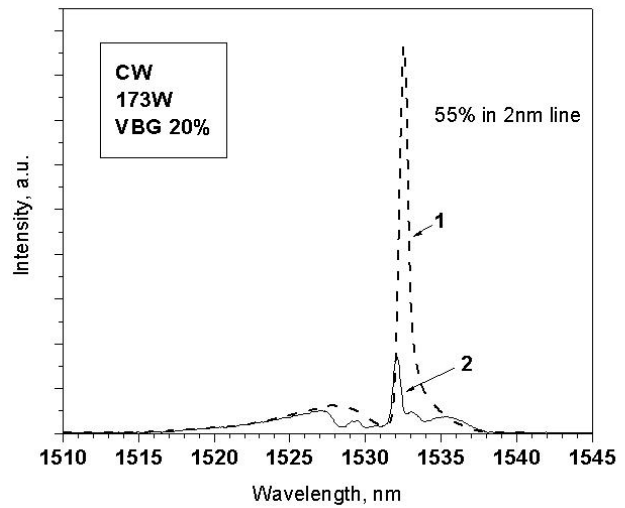


Fig. 5. Pump spectra before (1) and after the slab (2) for the VBG-narrowed InGaAsP/InP stack

that spectrally-selective feedback from VBG leads to significant redistribution of spectral power density from the stack without significant reduction of the stack power.

At 173 W of total stack power, about 55% is contained in a ~2-nm spectral range, which dramatically increases the fraction of the pump absorbed by Er^{3+} :YAG slab. Fig. 6 displays the VBG-narrowed InGaAsP/InP stack spectra also taken before and after the Er^{3+} :YAG slab at significantly lower stack current and, hence, output power. At 65 W (as opposed to ~173 W in Fig. 5) the fraction of total power contained in the line increases up to 77%. In this case the fraction of the pump absorbed by the Er^{3+} :YAG slab will become even higher with respect to that shown in Fig. 5. A lower fraction of the total pump power contained in the line in Fig. 5 can be explained by a combination of the weak feedback from the VBG (seen by the stack) and the trend of spectral widening at higher currents through the InGaAsP/InP stack. VBG feedback is weak because the coupling efficiency of the VBG-reflected light into individual emitters of the stack is much less than 100%. The choice of a proper effective VBG reflectivity is a trade off between the required efficient line-narrowing and loss of stack power caused by VBG reflection. In our case, at 20% VBG reflectivity, the reduction in total stack power upon spectral narrowing at ~180 W power level did not exceed 7%.

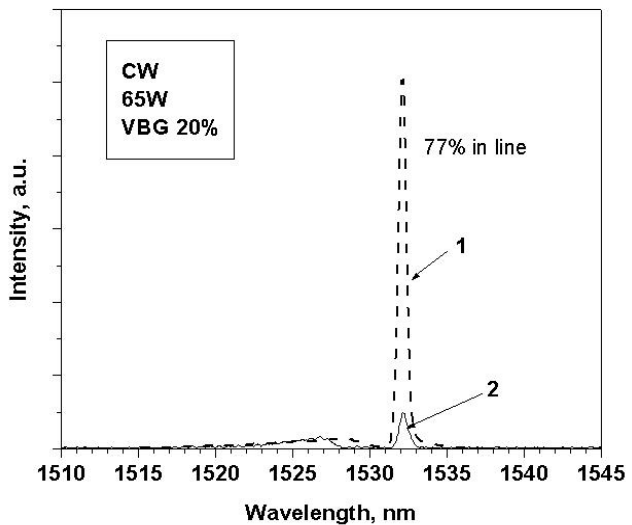


Fig. 6. Pump spectra (1) before and (2) after the slab for the VBG-narrowed InGaAsP/InP stack at low power.

The VBG spectrum stabilization and narrowing will significantly affect the absorbed fraction of pump power in the slab, as is clearly demonstrated in Fig. 7. Curve 1 shows the absorbed fraction of pump power versus incident pump power for the VBG-stabilized stack. Curve 2 illustrates a similar dependence for the stack without the VBG. Curve 3 corresponding to the scale on the right indicates the ratio of the values from curves 1 and 2. All these dependencies were measured without the mirror M2 (Fig. 2), i.e., they correctly reflect the gain medium behavior before the

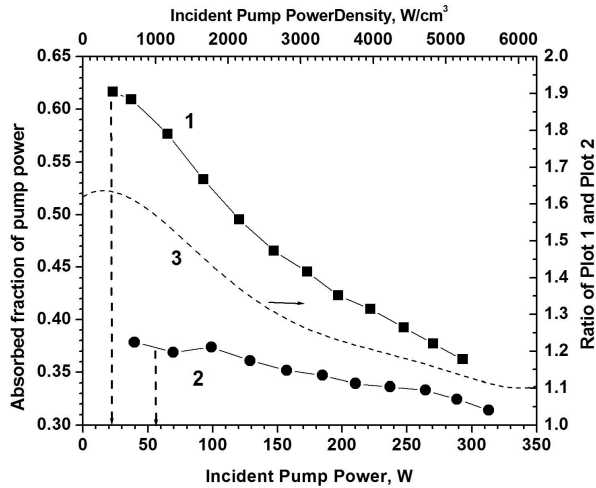


Fig. 7. Absorbed fraction of pump power for VBG-narrowed InGaAsP/InP stack (curve 1) and without VBG (curve 2) versus incident pump power (bottom scale) and incident pump power density (top scale). Curve 3 on the right-hand scale displays the ratio of curve 1 and curve 2.

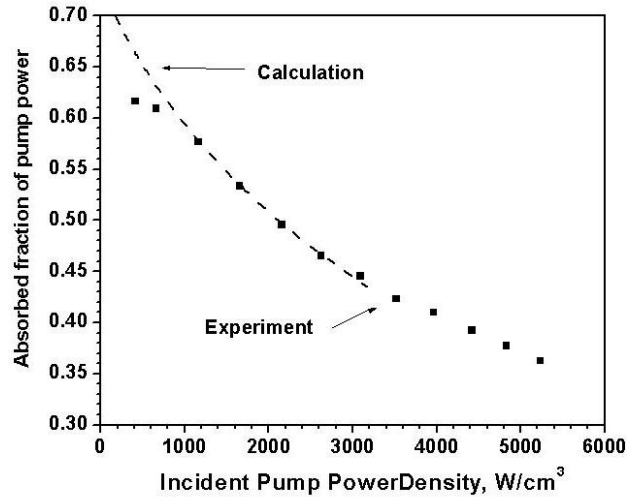


Fig. 8. Comparison of calculated absorbed fraction of pump power in 1532.5 nm line and experimental data obtained for VBG-stabilized stack versus incident power

threshold. It is clear that the absorbed fraction of pump power after the threshold will remain constant (assuming there are no severe thermal effects). The top scale shows the incident power density calculated from the estimated pumped volume of 0.056 cm^3 .

As seen from Fig. 7, the absorbed fraction of pump power for the VBG-stabilized pump source is always higher than that for the source without VBG stabilization. In the low incident power range, the absorbed fraction is 1.6 times higher for the VBG-stabilized pump source. However, VBG-stabilized pump power no longer offers such a significant advantage at much higher incident pump power. There are two reasons for this. First, as mentioned earlier, the pump source spectrum is wider at higher power levels and the stabilization/narrowing effect of the VBG becomes less efficient (as is also seen from Fig. 5 and Fig. 6). Surely, reduction of the power fraction in a $\sim 2 \text{ nm}$ -wide line is partially compensated by absorption in the adjacent absorption lines. The second factor, which reduces the absorption at high incident power, is caused by ground-state population depletion effect (bleaching). Based on the theory by R. Beach [11], we calculated the absorption versus incident power (for an “ideally-stable” 1532.5 nm pump source) in order to estimate the contribution of bleaching in the above experimental results.

Comparison of the calculated absorbed fraction of pump power in the 1532.5 nm line and experimental data obtained for VBG-stabilized stack versus incident power is shown in Fig. 8. This comparison leads to the conclusion that the bleaching effect clearly dominates in our experimental conditions. Therefore, in order to fully utilize the advantages of pump spectral narrowing by VBG, it is important to work in the low threshold power density range. The cumulative effect of pump spectrum stabilization and narrowing on the performance of resonantly-pumped Er^{3+} :YAG DPSSL is demonstrated in Fig. 9. The CW output power of Er^{3+} :YAG DPSSL versus incident pump power for the VBG-stabilized pump source (solid squares) and pump source without VBG (hollow squares) are measured with a 4% output coupler. The comparison in Fig. 9 demonstrates significant improvement of the Er^{3+} :YAG DPSSL performance by spectrally narrowing the pump. Slope efficiency increased 1.7 times and threshold power decreased 2.5 times. Output power is doubled for incident pump powers up to 200W. Linearity of the output power versus incident pump power dependence in this range corroborates our assumption that reduction of the absorbed fraction of pump power at higher incident pump powers is caused by the bleaching effect. In a range of incident powers beyond 200W, the use of VBG-stabilized InGaAsP/InP stack is less advantageous due to thermal effects in the slab and the increasing effective width of the pump source. The maximum output power achieved in our experiments was 51W and 31W for Er^{3+} :YAG DPSSL with the VBG-narrowed InGaAsP/InP pump and the pump without VBG, respectively.

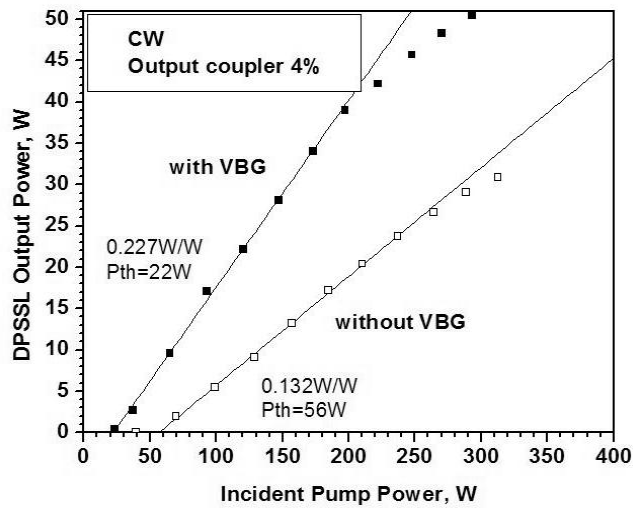


Fig. 9. Er^{3+} :YAG DPSSL output power versus incident pump power for VBG stabilized the ten arrays stack (solid squares) and pump source without VBG (hollow squares). Output coupler: $T = 4\%$.

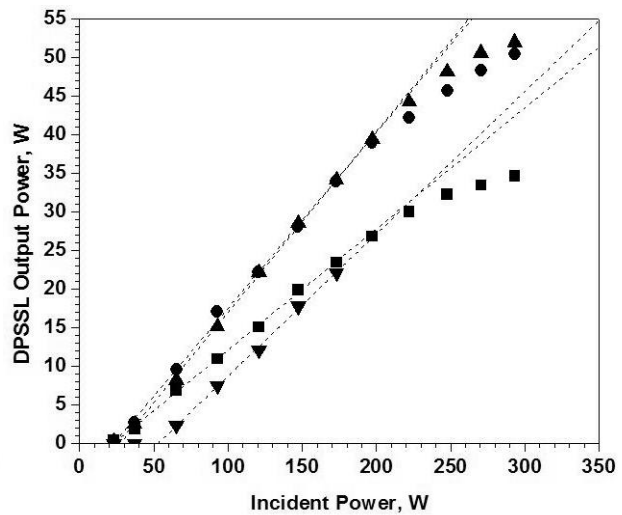


Fig. 10. Er^{3+} :YAG DPSSL output power versus incident pump power at output coupler $T = 2\%$ (solid squares), $T=4\%$ (solid circles), $T = 7\%$ (upward solid triangles), $T=15\%$ (downward solid triangles) for the VBG-narrowed pump.

Fig. 10 shows the Er^{3+} :YAG DPSSL output power versus incident pump power for a set of different output couplers: $T=2\%$ (solid squares), $T=4\%$ (solid circles), $T=7\%$ (solid upward triangles) and $T=15\%$ (solid downward triangles). It is clear that the optimum outcoupling loss resides in the range of 4 - 7%.

This is best illustrated by Fig. 11, which indicates the absorbed threshold power and slope efficiency (per absorbed power) versus output coupling loss (%). In the 4% to 7% outcoupling loss range slope efficiency has a relatively narrow plateau wherein the threshold power does not increase enough to degrade the SSL performance. The slope efficiency in that range is about 0.37 - 0.38 per absorbed power (it corresponds to about 40% photon-to-photon efficiency).

Higher spectral brightness due to VBG use allows decreasing the number of arrays in the pump stack. A lower number of pump arrays is desirable because it gives a narrower waist in the plane perpendicular to the slab (stable direction in hybrid resonator), which improves mode overlapping. In turn, better mode overlapping leads to the increase of slope efficiency. An additional advantage of decreasing the quantity of arrays is that, in practice, it is much easier to establish stronger feedback from the VBG, which means weaker spectrum sensitivity to array drive current or to operational temperature.

To demonstrate the advantage of reducing the number of pump arrays, we replaced the ten-array stack by one array (see Fig 2). In Fig. 11 the absorbed threshold power and slope efficiency (per absorbed power) indicated by open squares and triangles are shown versus output coupling loss (%) for a DPSSL with the VBG-narrowed single array. As seen from the figure, the optimum outcoupling loss range is similar to that found with a stack, and it is between 4% and 7%. The slope efficiency in that range is about 0.41-0.42 per absorbed power, corresponding to about 45% photon-to-photon efficiency.

Figure 12 shows the dependence of the output power of the DPSSL with a 4% output coupler on the incident pump power from a one-array pump source. For this experiment, we did not adjust the temperature of the array. Comparison with the results shown in Fig. 9 demonstrates a significant improvement in performance. The incident threshold power was reduced 2.9 times. The slope efficiency increased 1.3 times. The DPSSL pumped by a single array without VBG exhibited over 2.5 times power decrease for all range of incident powers. The measured absorbed fraction of the incident power was 70% for one VBG stabilized array, which is about 8% higher than that for the VBG stabilized stack used initially. Therefore, a better waist provided clear performance improvements.

The hybrid resonator shown in Fig. 3 was used to get good beam quality. A seven-array stack was selected as a pump source to provide a smaller waist in the stable direction compared with the waist in experiments with the ten-array stack. We used QCW pumping for this experiment because CW pumping demands several stacks to create a uniform pump power distribution in the plane of the slab with a lateral size significantly higher than the thickness of the slab.

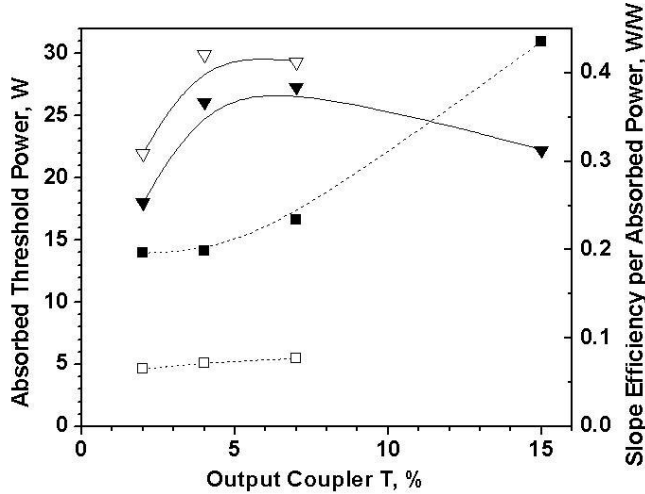


Fig. 11. Absorbed threshold power (ten arrays stack: solid squares, one array: open squares) and slope efficiency (ten arrays: solid downward triangles, one array: open downward triangles) per absorbed power versus output coupler transmission.

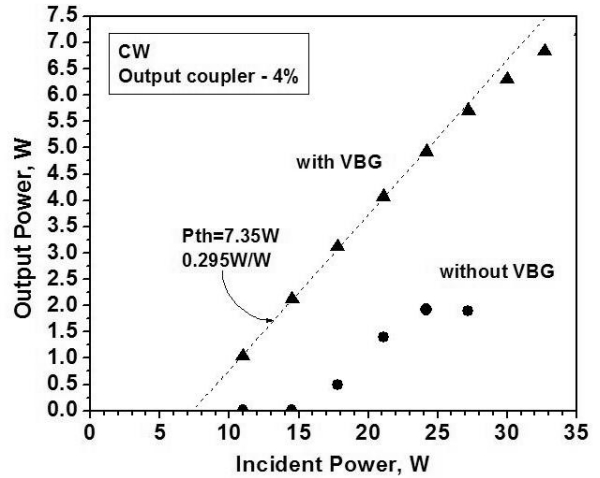


Fig.12. Er^{3+} :YAG DPSSL output power versus incident pump power for VBG stabilized single array (solid triangles) and pump source without VBG (solid circles). Output coupler: $T=4\%$

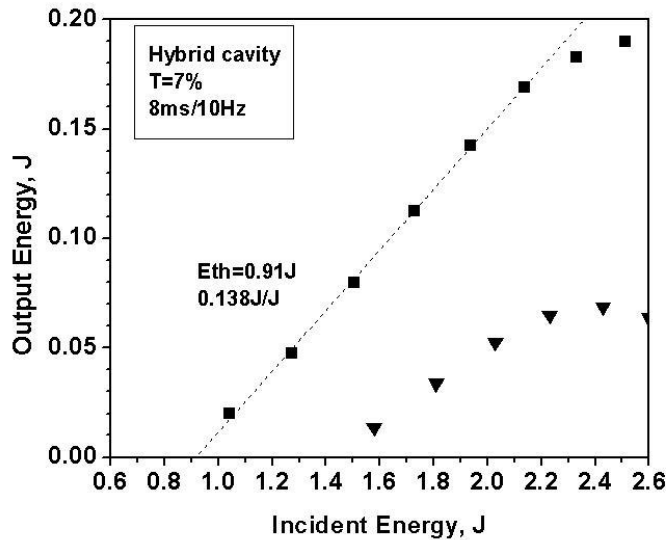


Fig. 13. Er^{3+} :YAG DPSSL output energy versus incident pump energy for VBG stabilized the seven arrays stack (solid squares) and pump source without VBG (solid downward triangles). Hybrid cavity, output losses: $T=7\%$

The output energy in a single pulse of the Er^{3+} :YAG DPSSL versus incident pump energy for the VBG-stabilized pump source (solid squares) and pump source without VBG (solid down triangles) are shown in Fig. 13. The DPSSL with the VBG-stabilized pump source demonstrates superior characteristics compared with the non-stabilized pump source. An output energy increase by more than a factor of 2.5 was observed when using the VBG. The slope efficiency was 0.138

J/J and the threshold energy was about 0.91 J for this configuration. This performance is worse than that of the stable configuration. It is caused by pump spectrum widening in pulse operation. We measured the absorption to be about 43% of the pump power. About 180 mJ pulse output energy was obtained with a beam quality of $M^2 = 1.3$ in stable direction and $M^2 = 1.1$ in unstable direction.

4. CONCLUSION

We reported significant CW performance improvement of a resonantly pumped Er:YAG solid state laser at 1.645- μm with direct pumping by a 1530-nm InGaAsP/InP FAC/SAC diode bar stack or single diode array. This improvement has been achieved by implementation of VBG stabilization and spectral narrowing of the bar stack or single diode array spectra. Incident Er:YAG CW threshold power has been reduced by a factor of 2.5, and the optical efficiency has been increased by a factor of 1.7, resulting in a slope efficiency of ~23% for stack and ~30% for single array per incident power. We demonstrated the importance of keeping the laser in the low threshold power density range in order to be able to take full advantage of VBG stabilization. In the optimum range of output coupling loss (4 - 7%), the absorbed threshold power was 14 – 17 W for the stack and about 5 W for the single array; slope efficiency was ~0.37 - 0.38 for the stack and ~0.41 - 0.42 for the single array per absorbed pump power. We obtained over 51 W of CW power in our experiments, which is, to the best of our knowledge, the highest CW power ever obtained from the resonantly-pumped Er:YAG laser with direct diode pumping. In QCW more than 180 mJ output energy per pulse was obtained in the stable-unstable or hybrid resonator with a beam quality of $M^2 = 1.3$ in the stable direction and $M^2 = 1.1$ in the unstable direction. The measured slope efficiency was 0.138 J/J and threshold energy 0.91 J.

This work was partially supported by the HEL-JTO/AF through Contract No. FA9451-04-C-0189. The authors acknowledge M. Itzler for creative discussions.

REFERENCES

1. N. Agladze, M. Popova, E. Vinogradov, T. Murina, V. Zhekov, "Oscillator Strength in $\text{Y}_3\text{Al}_5\text{O}_{12}\text{-Er}^{+3}$," *Opt. Commun.* **65**, p 351, (1988).
2. T. Schweizer, T. Jensen, E. Heumann, G. Huber, "Spectroscopic Properties of Yb: Er:YAG," *Opt. Commun.* **118**, p. 557, (1995).
3. S. D. Setzler, M. P. Francis, Y. E. Young, J. R. Konves, and E. P. Chicklis, "Resonantly pumped eyesafe erbium lasers," *IEEE Journal of Selected Topics in Quantum Electronics* **11**, 645-657 (2005).
4. D. Hogenboom, M. Nguyen, H. Chou, "Good Beam Quality From a Diamond-cooled Er:YAG laser," *Proc. of SPIE* **6216**, (2006)
5. D. Garbuzov, I. Kudryashov, M. Dubinskii, "110W (0.9J) pulsed power from resonantly diode-laser-pumped 1.6- μm Er:YAG laser", *Appl. Phys. Lett.* **87**, 121101 (2005)
6. P. Crump, T. Crum, M. DeVito, J. Farmer, M. Grimshaw, Z. Huang, S. Igl, J. Wang, W. Dong, "High Power 1470 nm Laser Bars and Stacks," *Technical Digest of SSDLTR 2004, Direct Energy Professional Society, Diode-3.*
7. D. Garbuzov, I. Kudryashov, A. Komissarov, "InGaAsP/InP Diode Laser Pumping Sources for Eye-Safe Solid-State and Fiber Lasers," *Optics East Conference*, paper 5594-37, (2004).
8. G. Venus, V. Smirnov, L. Glebov, and M. Kanskar, "Spectral Stabilization of Laser Diodes by External Bragg Resonator", *17th Annual Solid State and Diode Laser Technology Review, SSDLTR-2004 Technical Digest, Albuquerque, June 2004.*
9. M. Iskandarov, A. Nikitichev, A. Stepanov, "Quasi-two-level Er:YAG laser for 1.6 μm range," *J. Opt. Technol.*, **68** (12), p. 885 (2001).
10. K. Du, N. Wu, J. Xu, J. Gieseckus, P. Loosen, and R. Poprawe, *Opt. Lett.* **23**, 370 (1998).
11. R.J. Beach, "CW theory of quasi-three level end-pumped laser oscillators", *Opt. Commun.*, **123**, 385-393, (1995)